

## Investigation for mining-induced deformation in Upper Silesia Coal Basin with multi-GNSS in Near Real-Time

Damian Tondaś<sup>1</sup>, Kamila Pawłuszek<sup>1</sup>, Maya Ilieva<sup>1</sup>, Jan Kapłon<sup>1</sup>, Witold Rohm<sup>1</sup>

<sup>1</sup> Wrocław University of Environmental and Life Sciences, ([damian.tondas@upwr.edu.pl](mailto:damian.tondas@upwr.edu.pl))

**Key words:** *Near Real-Time; multi-GNSS; InSAR; subsidence; mine deformations*

### ABSTRACT

The EPOS-PL project is the Polish realization of the European Plate Observing System (EPOS) initiative, which has a main goal to integrate the existing and newly created research infrastructures to facilitate the use of multidisciplinary data and products in the field of Earth sciences in Europe. The structure of the project includes the construction and integration of research infrastructure in the local and national level, which, in turn, will lead the integration with European and global databases and services. One of the tasks in EPOS project is to create a service for continuous monitoring of GNSS station positioning in Near Real-Time (NRT) processing in areas affected by mining exploration. The NRT processing is carried out with a 15-minutes GNSS parameter estimation interval.

The mostly exposed region to the effects of deformation in Poland is the area of the Upper Silesian Coal Basin (USCB) in the southern part of the country. In this area is one of the largest coal deposits in Europe, where the exploitation has been carried out for the last 200 years. The mining works cause subsidence of the ground in the most populated area in Poland.

In order to conduct deformation research in this area, eight high-frequency GNSS receivers have been purchased within the EPOS-PL project. The NRT processing enables constant monitoring of the station locations. Depending on the duration of the surface deformation phenomenon (long-term – subsidence, short-term – earthquakes), it is possible to observe the coordinates changes. The displacements may occur not only in the vertical but also in the horizontal plane.

The paper depicts the results obtained in the research of multi-GNSS deformations in the USCB areas. The determined time series of coordinates have been analyzed for long-term and short-term effects of deformations. The long-term subsidence values are compared with the results obtained by advanced InSAR technique.

### I. INTRODUCTION

The main purpose of the EPOS project is to increase the availability and quality of research infrastructure in the field of Earth sciences. The extension of existing infrastructure will enable integration of results from various techniques. In the current study, we compare results obtained by Global Navigation Satellite Systems (GNSS) measurements and satellite interferometric radar (InSAR) data.

In Poland, the largest intensity of ground surface deformation occurs in the Upper Silesia region. In this area two research polygons, called Multidisciplinary Upper Silesian Episodes (MUSE) have been established (Figure 1).

As a part of the EPOS-PL research, the existing infrastructure on MUSE1 and MUSE2 polygons has been extended with new GNSS stations and corner reflectors which will be used in future for improving InSAR based deformation studies. The main purpose of this paper is the investigation for coal mining-induced deformation with multi-GNSS in Near Real-Time (NRT) system. As a reference to the GNSS NRT results we used natural persistent scatterers (PS) in advanced InSAR technique.

In the literature (Liu et al., 2018; Kadlečík et al., 2015), there are many examples of combining results from both GNSS and SAR techniques.

With respect to the published results by (Liu N. et al., 2018) the fusion of GNSS and InSAR techniques can be based on a dynamic filtering model to generate a high spatio-temporal resolution time series using Kalman filter method and, to densify InSAR measurements the authors used Hermite interpolating polynomial method in the temporal domain and the kriging method in the spatial domain. The kriging method was used also by (Kadlečík et al., 2015), to create the model of subsidence depressions of the GNSS values.

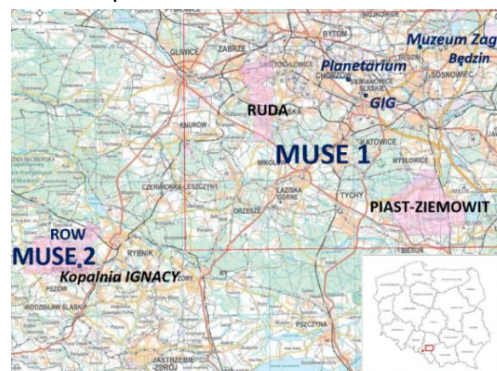


Figure 1. The location of MUSE polygons on the area of the Upper Silesian Coal Basin (Bosy et al., 2017)

Our interest is focused on the area of Rydułtowy mine located in MUSE2 polygon, where significant subsidence was expected. The predicted deformation zone caused by the extraction in this mine is limited to 30 km<sup>2</sup> and the results from only one GNSS station – RES1, can be discussed. The station is set on the roof of historic mine building, which is out of coal exploitation.

## II. DATA AND METHODOLOGY

### A. GNSS data and processing

The GNSS data were provided for a Near Real-Time GNSS network created for the EPOS-PL project purpose. The NRT service is based on Bernese GNSS Software v. 5.2 (Dach et al., 2015) with double-difference method. The interval of GNSS data processing was 15 minutes, whereas the data have been taken in 6-hour window observation. The NRT processing was based on the GPS and GLONASS system. The external products regarding orbits, satellite clocks and parameters of the Earth's rotation containing a short 24h prediction of these parameters were obtained from International GNSS Service (IGS) data bases (Springer and Hugentobler, 2001).

The NRT calculation used observations from 33 stations situated on territory of Poland and neighborhood countries. Five from eight GNSS EPOS stations are located on the MUSE1 and MUSE2 areas. Three remaining stations have a control function and they are located on areas not exposed to influence of subsidence (Figure 2). The ITRF2014 reference frame is introduced using the 25 stations belonging to the IGS and EUREF Permanent GNSS Network (EPN) networks (Bosy et al., 2009).

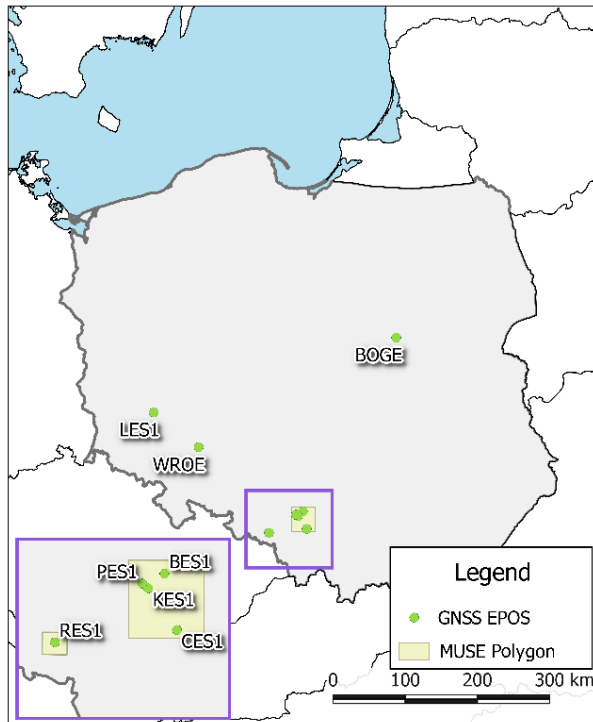


Figure 2. The location of GNSS stations purchased within the EPOS-PL project

For each epoch of estimations, parameters defining the troposphere state (Zenith Total Delay, Zenith Wet Delay, horizontal gradients) and coordinates of particular stations participating in the solution were determined. The NRT processing was started on 5/12/2018 using the ITRF2014 frame as a reference. In order to determine whether the movement of station is significant, the coordinates in the ITRF2014 reference frame were converted to the ETRF2014 reference frame at the same epoch (Altamimi, 2017) following the equations (1,2):

$$X_{yy}^E(t) = X_{yy}^I(t) + T_{yy} + R \cdot X_{yy}^I(t) \cdot (t - 1989.0) \quad (1)$$

where  $X_{yy}^E(t)$  = the station position in the yy realisation of the ETRS89 system  
 $X_{yy}^I(t)$  = the station position in the yy realisation of the ITRS system  
 $T_{yy}$  = the translation vector  
 $R$  = the rotation matrix (2)  
 $t$  = the epoch

$$R = \begin{bmatrix} 0 & -R\dot{3}_{yy} & \dot{R}_2 \\ R\dot{3}_{yy} & 0 & -R\dot{1}_{yy} \\ -R\dot{2}_{yy} & R\dot{1}_{yy} & 0 \end{bmatrix} \quad (2)$$

where  $R\dot{1}_{yy}, R\dot{2}_{yy}, R\dot{3}_{yy}$  = the rotation rate parameters between ITRS and ETRS89

However, InSAR measurements have specifics – their results include the continental movement. It is impossible to eliminate the influence of the Eurasian Plate displacement. Therefore, the comparison between GNSS and SAR results is based on the ITRF2014 reference frame.

Furthermore, to compare the results from both techniques, the XYZ geocentric coordinates have been converted to the topocentric North-East-Up reference frame (NEU) (Bogusz and Figurski, 2010) using the equation (3):

$$\begin{bmatrix} N \\ E \\ U \end{bmatrix} = r \cdot \begin{bmatrix} T_X \\ T_Y \\ T_Z \end{bmatrix} \quad (3)$$

where  $N, E, U$  = the station position in the local topocentric reference frame  
 $r$  = the rotation matrix (4)  
 $T_X, T_Y, T_Z$  = coordinates differences (5)

The rotation matrix is using the geodetic geocentric coordinate system coordinates (4):

$$r = \begin{bmatrix} -\sin(\varphi) \cos(\lambda) & -\sin(\varphi) \sin(\lambda) & \cos(\varphi) \\ -\sin(\lambda) & \cos(\lambda) & 0 \\ \cos(\varphi) \cos(\lambda) & \cos(\varphi) \sin(\lambda) & \sin(\varphi) \end{bmatrix} \quad (4)$$

where  $\varphi$  = latitude  
 $\lambda$  = longitude

Equation (5) shows the vector containing the differences between geodetic geocentric coordinates of a reference point and a single point in time series:

$$\begin{bmatrix} T_X \\ T_Y \\ T_Z \end{bmatrix} = \begin{bmatrix} X_p \\ Y_p \\ Z_p \end{bmatrix} - \begin{bmatrix} X_0 \\ Y_0 \\ Z_0 \end{bmatrix} \quad (5)$$

where  $X_p, Y_p, Z_p$  = the coordinates of single point  
 $X_0, Y_0, Z_0$  = the coordinates of reference point

Based on the designated NEU topocentric positions, it is possible to determine the station velocity for each north, east and up directions. To limit the influence of outliers on the final results the M-estimation method was used. This method was introduced by Huber (1964) and is the most common general method of robust regression. Determination of model parameters and equalization of observations is carried out following the approach of the least squares method (LSM), but with the difference that in the LSM method the influence of gross errors is not eliminated. With the usage of the M-estimation method it is possible to reduce the impact of some observations by appropriate weighting. It is an iterative method, for which in each iteration a new weight matrix is created and the weights of observations with gross errors are getting smaller (Chang and Guo, 2005).

In this study a M-estimation model for which the parameters are linearly dependent of time was applied (6):

$$Y(t_i) = v \cdot t_i + b \quad (6)$$

where  $Y(t_i)$  = the coordinate value for  $t_i$  epoch  
 $v$  = the velocity  
 $t_i$  = the epoch  
 $b$  = the initial position of point

### B. InSAR data and processing

In this study, 30 Sentinel-1 SAR images (C-band) in descending mode from the relative satellite number of 51 acquired over the Rydułtowy mine were selected to estimate subsidence caused by mining activity. The data cover the time span from the beginning of August 2017 up to the end of January (29th) 2019. More detailed information can be found in the table below.

Table 1. SAR data specifications for the Rydułtowy Study area

Orbit direction	descending
Track number	51
Number of acquisitions	30
Date of first acquisition	1 August 2018
Date of last acquisition	29 January 2019
Sensor	Sentinel 1A+1B
Product type	SLC IW
Mean incidence angle on the study area (degree)	44.04
Azimuth angle (degree)	-78.97
Polarization	VV

In presented study, we applied classical PSInSAR approach presented by (Ferreti et al., 2000; 2001). This technique was developed to employ the persistent scatterers (PS). These are scatterers, which sizes are smaller than the resolution cell of SAR image (Ferretti et al., 2001). Therefore, this approach has considerable advantage that PS points are not affected by baseline decorrelation. This means that all acquired data can be used to create interferograms even where the baseline is longer than critical baseline. Using this technique, it is possible to achieve sub-meter precision of Digital Elevation Model (DEM) formation and a deformation precision of a few millimeters (Ferretti et al., 2007b).

The baseline configuration between the images used in this study is presented in Figure 3. The three-arc-second Shuttle Radar Topography Mission (SRTM) DEM provided by the National Aeronautics and Space Administration (NASA) was used to remove topographic phase component. Precise Orbit Determination (POD) data provided by European Space Agency were applied to the orbital refinement and phase re-flattening.

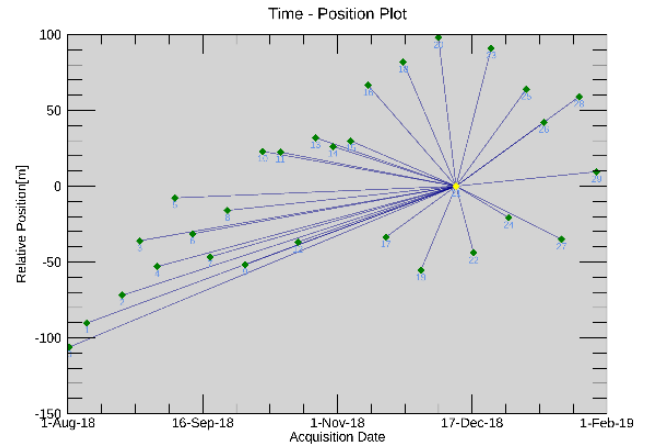


Figure 3. Baseline configuration between slaves and master image

## III. RESULTS

### A. GNSS Results

The velocity determination was based on a 4-month observation period. Acquired GNSS data cover the time span from 5<sup>th</sup> of December 2018 up to 4<sup>th</sup> of March 2019. The annual displacement velocities for RES1 station in the N, E, U directions in the ITRF2014 reference frame are 8.3, 1.4, -4.5 cm/year, respectively. The calculated values include the station movement and the Eurasian Plate drift. After eliminating the influence of the continental plate, the station motion reached up to 6.8 cm/year in the North direction, -0.7 cm/year in the East direction and -4.5 cm/year in the Up direction.

The time series of station position and estimated velocities is presented on Figure 4.

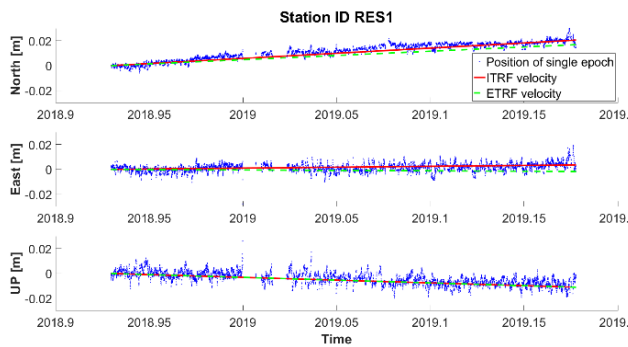


Figure 4. The estimated topocentric positions and velocities in ITRF2014 and ETRF2014 reference frames

The Figure 5 presents horizontal and vertical movements of RES1 station, determined in the ETRF2014 reference frame and seismic episodes from November 2018 to March 2019. The earthquake with the largest magnitude of 3.4 was registered 22/01/2019 in the north direction to the station. The existing episodes are related to the ongoing coal exploitation.

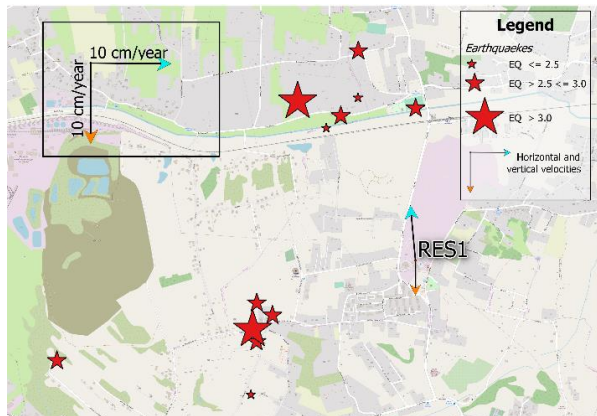


Figure 5. The visualization of horizontal and vertical velocities of RES1 station and the location of seismic episodes from November 2018 to March 2019

#### B. InSAR results

The results for the PSInSAR processing have been presented in Figure 6. It can be observed that within the study area of MUSE2, three subsidence basins exist. The subsidence values detected by PSInSAR reach up to 20 cm since 1<sup>st</sup> of August 2018 to 29<sup>th</sup> January 2019. Due to the temporal decorrelation, some information within the center of subsidence basins is missing. Nevertheless, the EPOS-PL GNSS RES1 station is located at the border of one of the subsidence basins, where the deformation velocity was able to capture using PSInSAR approach.

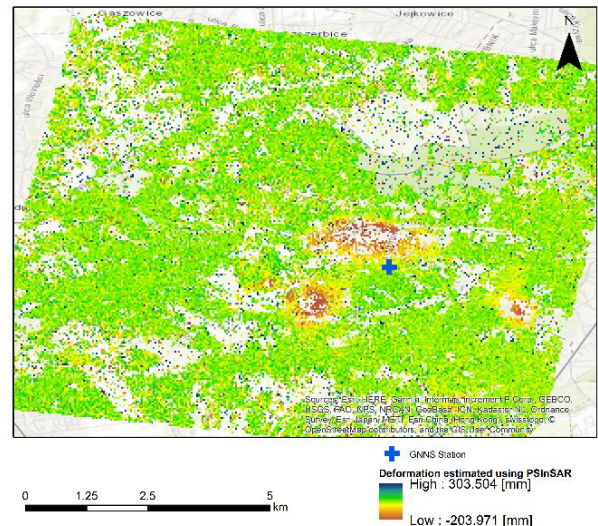


Figure 6. Deformation estimated using PSInSAR approach for the time span 1.08.2018 - 29.01.2019

#### IV. GNSS AND PSINSAR COMPARISON

The proposed GNSS processing approach shows stable solution in the areas of intensive mining exploitation. The results are validated by a comparison with PSInSAR results. For that purpose, the 10 nearest to the RES1 GNSS station PS points were selected. Eight of the points are located on the building, while the other two are situated outside the contour of the building (Figure 7).

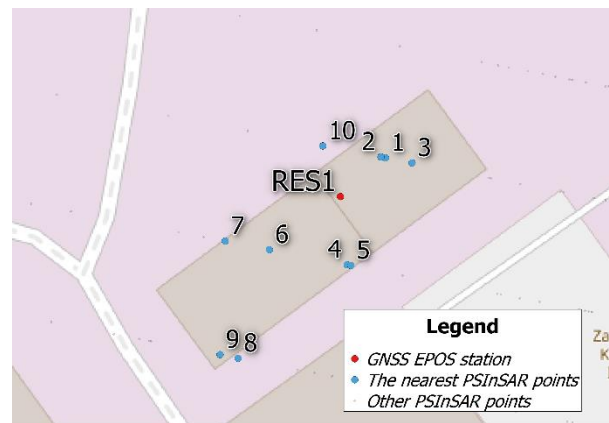


Figure 7. The location of the 10 nearest PSInSAR points with respect to the RES1 station

A comparative analysis of their time series with the one of the GNSS station is performed. In order to compare the deformation value from both techniques, it was necessary to convert the NEU GNSS values into a displacement towards the SAR satellite along the line-of-sight (LOS). To accomplish this task, the following relation was used (7):

$$Z_{los} = [\sin(\theta_{inc})\sin(\alpha) - \sin(\theta_{inc})\cos(\alpha) \cos(\theta_{inc})] \begin{bmatrix} N \\ E \\ U \end{bmatrix} \quad (7)$$

where  $Z_{los}$  = the deformation in direction of line-of-sight  
 $\theta_{inc}$  = the radar incidence angle  
 $\alpha$  = the azimuth angle of Sentinel-1 flight  
 $N, E, U$  = the station position in the local topocentric reference frame

Overlapping periods of observations performed by GNSS and PSInSAR measurements were extracted for the period from 5<sup>th</sup> of December 2018 to 21<sup>st</sup> of January 2019. The results of the comparison between both techniques are presented for two chosen points in Figure 8 and Figure 9. The M-estimation approach was used to determine the parameters of the deformation velocity towards LOS direction for each method.

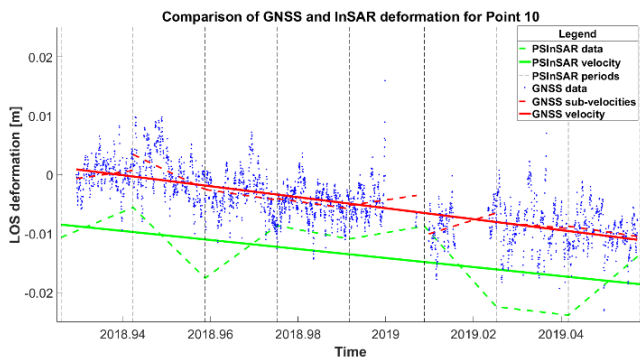


Figure 8. The comparison between GNSS and PSInSAR deformation for Point 10

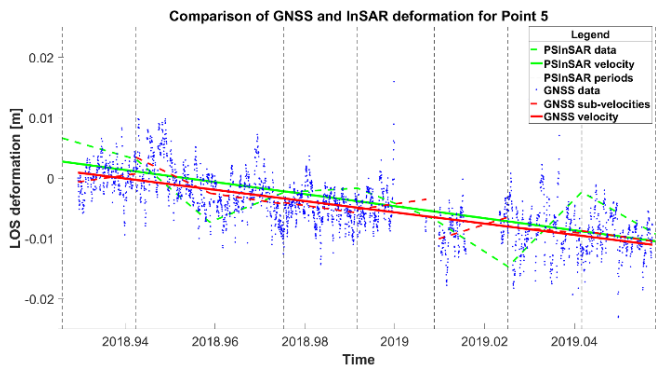


Figure 9. The comparison between GNSS and PSInSAR deformation for Point 5

The results characterized by grater shift of velocities were obtained to point 10, which is located outside the building contour. The shift reaches up to 1 cm, while the velocities are  $-9.3$  cm/year for RES1 station and  $-7.7$  cm/year for point 10. The average standard deviation is  $-4$  mm/year and  $-7$  mm/year respectively.

The most similar results for both techniques are found for point 5, which is situated on the edge of building. For this data time series, the shift is close to 0 cm/year and the velocities reach up  $-10.0$  cm/year for point 5. The average standard deviation 5 mm/year.

Additionally, the GNSS station is located in the border of the subsidence basin. Point 10 is located closer to the epicenter of the subsidence basins. Moreover, another reason for this could be, the geometry of the Sentinel sensors. Namely, slant range geometry and near polar orbit constellation, which is insensitive to detect North-South displacement component.

## V. CONCLUSIONS

Deformations caused by mining industry are a significant problem, especially in areas characterized by high population density. Continuous monitoring over the effects of mining expansion is possible using many measurement techniques, among which are GNSS precise positioning and SAR technology.

The NRT processing enables constant monitoring of the stations location, while PSInSAR technique using the SENTINEL-1 two-satellite constellation offers a 6 day exact repeat cycle. However, the integrated use of GNSS and SAR measurements enables to extend the concept of safety monitoring in spatiotemporal mode.

Thanks to the comparison of GNSS and PSInSAR results, this paper proved the effectiveness of both techniques for subsidence monitoring. The GNSS measurements are capable to detect displacements in all directions while the specificity of the SAR technique makes it impossible to detect displacements in the north-south directions.

From another point of view, PSInSAR provide bigger spatial coverage in comparison to single point of GNSS station. Therefore, both methods should be jointly applied in order to capture comprehensive information about the deformation pattern.

The conversion of GNSS displacements in North East, Up directions allows to compare with InSAR deformations by the line of sight to the satellite.

## References

- Altamimi, Z. (2017). EUREF Technical Note 1: Relationship and Transformation between the International and the European Terrestrial Reference Systems. Institut National de l'Information Géographique et Forestière (IGN), France.
- Bogusz, J., & Figurski, M. (2010). Short-period information in GPS time series. *Artificial Satellites*, 45(3), 119-128.
- Bosy, J., Kontny, B., & Borkowski, A. (2009). IGS/EPN reference frame realization in local GPS networks. In *Geodetic Reference Frames* (pp. 197-203). Springer, Berlin, Heidelberg.
- Bosy, J., et al. (2017). Research Infrastructure EPOS-PL Buildin framework of EPOS –European Plate Observing System Co-financed under Action 4.2: Development of modern research infrastructure of the science sector in the Operational Program Smart Growth
- Chang, X. W., & Guo, Y. (2005). Huber's M-estimation in relative GPS positioning: computational aspects. *Journal of Geodesy*, 79(6-7), 351-362.
- Dach, R., S. Lutz, P. Walser, and P. Fridez, eds. 2015. *Bernese GNSS Software Version 5.2 User Manual*. Astronomical Institute, University of Bern.

Ferretti, A., Prati, C., & Rocca, F. (2000). Nonlinear subsidence rate estimation using permanent scatterers in differential SAR interferometry. *IEEE Transactions on geoscience and remote sensing*, 38(5), 2202-2212.

Ferretti, A., Prati, C., & Rocca, F. (2001). Permanent scatterers in SAR interferometry. *IEEE Transactions on geoscience and remote sensing*, 39(1), 8-20.

Ferretti, A., Savio, G., Barzaghi, R., Borghi, A., Musazzi, S., Novali, F., ... & Rocca, F. (2007). Submillimeter accuracy of InSAR time series: Experimental validation. *IEEE Transactions on Geoscience and Remote Sensing*, 45(5), 1142-1153.

Huber, P. J. (1964). Robust Estimation of a Location Parameter. *The Annals of Mathematical Statistics*, 35(1), 73-101.

Kadlečík, P., Kajzar, V., Nekvasilová, Z., Wegmüller, U., & Doležalová, H. (2015). Evaluation of the subsidence based on dInSAR and GPS measurements near Karvina, Czech Republic. *AUC Geographica*, 50(1), 51-61.

Liu, N., Dai, W., Santerre, R., Hu, J., Shi, Q., & Yang, C. (2018). High Spatio-Temporal Resolution Deformation Time Series With the Fusion of InSAR and GNSS Data Using Spatio-Temporal Random Effect Model. *IEEE Transactions on Geoscience and Remote Sensing*, (99), 1-17.

Springer, T. A., and U. Hugentobler. 2001. "IGS Ultra Rapid Products for Near-Real-Time Applications." *Physics and Chemistry of the Earth, Part A: Solid Earth and Geodesy*.